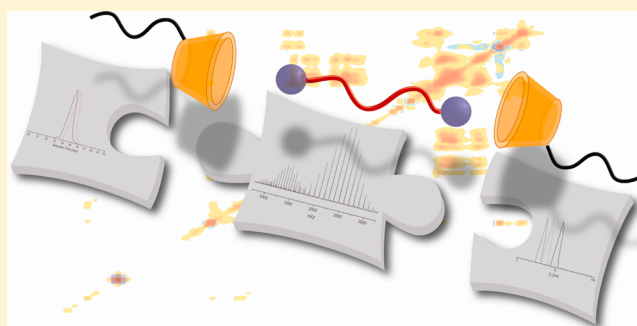


## UV Light and Temperature Responsive Supramolecular ABA Triblock Copolymers via Reversible Cyclodextrin Complexation

Bernhard V. K. J. Schmidt,<sup>†</sup> Martin Hetzer,<sup>‡</sup> Helmut Ritter,<sup>\*,‡</sup> and Christopher Barner-Kowollik<sup>\*,†</sup><sup>†</sup>Preparative Macromolecular Chemistry, Institut für Technische Chemie und Polymerchemie, Karlsruhe Institute of Technology (KIT), Engesserstr. 18, 76128 Karlsruhe, Germany<sup>‡</sup>Lehrstuhl für Präparative Polymerchemie, Institut für Organische Chemie und Makromolekulare Chemie, Heinrich-Heine Universität, Universitätsstrasse 1, Geb. 26.33.00, 40225 Düsseldorf, Germany

## Supporting Information

**ABSTRACT:** A novel triblock macromolecular architecture based on cyclodextrin (CD) complexation is presented. A CD-functionalized biocompatible poly(*N*-(2-hydroxypropyl)methacrylamide) (PHPMA) building block ( $3800 \leq M_n \leq 10\,600 \text{ g mol}^{-1}$ ;  $1.29 \leq D_M \leq 1.46$ ) and doubly guest-containing poly(*N,N*-dimethylacrylamide) (PDMAAm) ( $6400 \leq M_n \leq 15\,700 \text{ g mol}^{-1}$ ;  $1.06 \leq D_M \leq 1.15$ ) and poly(*N,N*-diethylacrylamide) (PDEAAm) ( $5400 \leq M_n \leq 12\,100 \text{ g mol}^{-1}$ ;  $1.11 \leq D_M \leq 1.33$ ) segments were prepared via reversible addition–fragmentation chain transfer (RAFT) polymerization and subsequently utilized for the formation of a well-defined supramolecular ABA triblock copolymer. The block formation was evidenced via dynamic light scattering (DLS), nuclear Overhauser effect spectroscopy (NOESY), and turbidity measurements. Furthermore, the connection of the blocks was proven to be temperature responsive and—in the case of azobenzene guests—responsive to the irradiation with UV light. The application of these stimuli leads to the disassembly of the triblock copolymer, which was shown to be reversible. In the case of PDEAAm containing triblock copolymers, the temperature-induced aggregation was investigated as well.



## INTRODUCTION

Complex macromolecular architectures constitute an important field in contemporary polymer chemistry. Block copolymers belong to the most studied materials in this field and are subjected to manifold applications.<sup>1,2</sup> Apart from classical anionic<sup>3</sup> and cationic<sup>4</sup> polymerization, living controlled radical polymerizations, e.g., nitroxide-mediated radical polymerization,<sup>5</sup> atom transfer radical polymerization,<sup>6,7</sup> and reversible addition–fragmentation chain transfer (RAFT) polymerization,<sup>8,9</sup> have proven to be a very versatile tool for the generation of new block copolymers with a large variety of different blocks via convenient synthetic procedures. Furthermore, click chemistry had a strong impact on the field of block copolymer synthesis,<sup>10–12</sup> e.g., via the copper(I)-catalyzed azide–alkyne cycloaddition (CuAAC),<sup>13</sup> the Diels–Alder,<sup>14</sup> or the RAFT hetero-Diels–Alder reaction,<sup>15</sup> which provide numerous opportunities to generate block copolymers as well as more complex architectures.<sup>16,17</sup>

Cyclodextrins (CDs) gain more and more importance in polymer chemistry due to their ability to form noncovalent inclusion complexes with hydrophobic guest molecules, opening the opportunity to generate new supramolecular macromolecular architectures,<sup>18</sup> e.g., stars,<sup>19,20</sup> miktoarm stars,<sup>21,22</sup> hydrogels,<sup>23</sup> or polymer brushes.<sup>24</sup> Furthermore, CDs can be utilized to solubilize hydrophobic monomers<sup>25–28</sup>

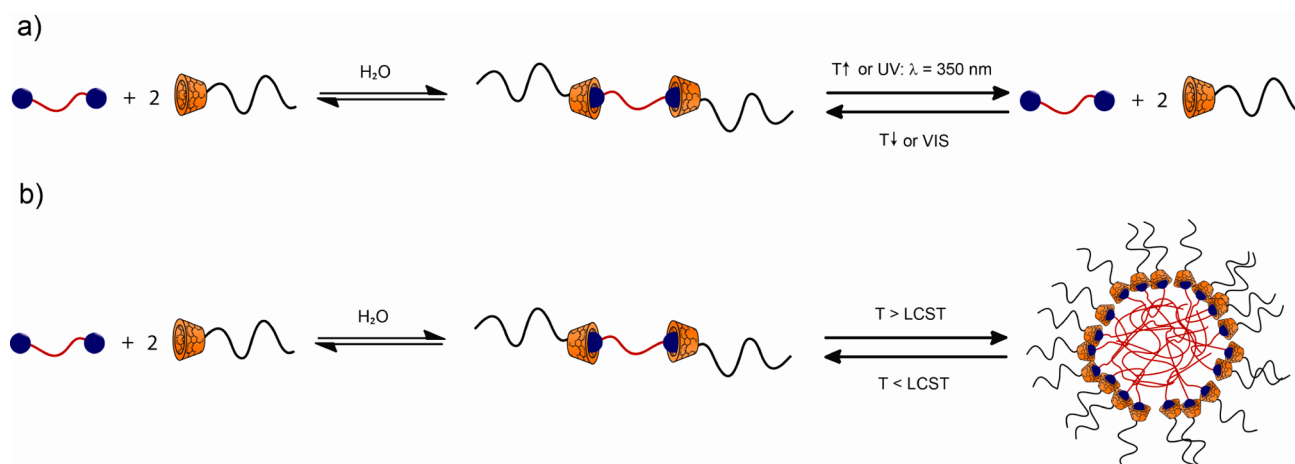
and chain transfer agents (CTAs)<sup>29</sup> in aqueous polymerizations. Recently, Harada and co-workers evidenced supramolecular interactions between host and guest containing gel cubes on a macroscopic scale which proves the powerful interactions between CDs and specific guest molecules.<sup>30</sup>

A further application of CDs in polymer chemistry is the utilization as a linker molecule for the formation of supramolecular block copolymers. Hereby, controlled radical polymerization techniques and click chemistry have proven to be a very powerful tool set for the incorporation of CD end groups into polymers. The most frequently applied click reaction is CuAAC due to the convenient synthesis of monoazido-functionalized  $\beta$ -CD ( $\beta$ -CD-N<sub>3</sub>). So far, mostly AB diblock copolymers with different properties have been described, e.g., with a light responsive linkage,<sup>31</sup> with a redox responsive linkage,<sup>32</sup> with a thermoresponsive block<sup>33</sup> and even with schizophrenic behavior of the blocks.<sup>34,35</sup> A further example is a CD-centered star polymer, where two cores are coupled using supramolecular interactions.<sup>36,37</sup> The variety of possible building blocks and guest moieties gives the opportunity for several applications. For example, light-

Received: November 19, 2012

Revised: January 19, 2013

Published: February 1, 2013

Scheme 1. Schematic Representation of the Formation of Supramolecular ABA Triblock Copolymers via CD Host/Guest Complexation<sup>a</sup>

<sup>a</sup> $\beta$ -CD is depicted orange; the guest groups are depicted blue; the outer PHPMA block is depicted black; the inner PDMAAm- and PDEAAm-blocks are depicted red. (a) PDMAAm based supramolecular block copolymers with temperature- and light-responsive complexation and (b) PDEAAm-based supramolecular block copolymers with cloud-point-triggered aggregate formation.

controlled supramolecular nanotubes have been described<sup>31</sup> as well as vesicular nanocontainers with voltage-triggered release<sup>32</sup> or the generation of dynamic core-shell nanoparticles.<sup>38</sup> A further example is a core-shell nanoassembly that shows tumor-triggered release.<sup>39</sup> One can imagine many applications that can be derived from conventional covalently bound block copolymers, e.g., self-assembly of supramolecular block copolymers coupled via hydrogen bonding motifs in thin films that mimic the behavior of their covalent role model.<sup>40</sup>

In our current approach, we connect two poly(*N*-(2-hydroxypropyl)methacrylamide) (PHPMA) outer blocks with a poly(*N,N*-dimethylacrylamide) (PDMAAm) or poly(*N,N*-diethylacrylamide) (PDEAAm) inner block via a CD host/guest complex to generate a novel supramolecular macromolecular architecture (see Scheme 1). We chose PHPMA due to its potential application in drug delivery.<sup>41</sup> PDMAAm was selected to study the thermoresponsive behavior of the host/guest complexation (refer to Scheme 1a), whereas PDEAAm was chosen due to its cloud point of close to 30 °C<sup>42</sup> and therefore close to physiological temperatures. The cloud point of PDEAAm can be utilized to form aggregates in aqueous solution upon heating that are connected via supramolecular interactions (see Scheme 1b).

Thus, we report the formation of a novel supramolecular ABA triblock copolymer consisting of a PDMAAm or PDEAAm inner block and a biocompatible PHPMA outer block. The inner building block was synthesized via RAFT polymerization employing novel doubly guest-functionalized CTAs featuring adamantyl or photoresponsive azobenzene guest groups. The outer building block was synthesized via RAFT polymerization with an alkyne containing CTA and subsequent CuAAC with  $\beta$ -CD- $N_3$ . The building blocks were characterized via <sup>1</sup>H NMR, electrospray ionization–mass spectrometry (ESI-MS), and size exclusion chromatography (SEC). The complex formation was investigated with dynamic light scattering (DLS), cloud point measurements, and nuclear Overhauser effect spectroscopy (NOESY).

## EXPERIMENTAL PART

**Materials.** 1-Adamantylamine hydrochloride (ABCR, 99%), 2-amino-1-propanol (TCI, 98%), 4,4'-azobis(4-cyanovaleric acid) (V-501; Sigma-Aldrich, 98%), 1-chloro-6-hydroxyhexane (Acros, 95%), 2-bromoisobutyric acid (Sigma-Aldrich, 98%), acetic acid (Roth, 99%), aluminum chloride (ABCR, 99%),  $\beta$ -cyclodextrin ( $\beta$ -CD; Wacker, pharmaceutical grade), carbon disulfide (Acros, 99.9%), copper bromide (Sigma-Aldrich, 99%), diisopropylazodicarboxylate (DIAD; ABCR, 94%), *N,N'*-dicyclohexylcarbodiimide (DCC; ABCR, 99%), *N,N*-dimethylaminopyridine (DMAP; Sigma-Aldrich, 99%), *N,N*-dimethylformamide (DMF; ABCR, 99%),  $\epsilon$ -caprolactone (Alfa Aesar, 99%), ethanethiol (Acros, 99%), ethylenediaminetetraacetic acid disodium salt (EDTA; ABCR, 99%), iodine (Acros, 99.5%), 3-mercaptopropionic acid (Acros, 99%), methacryloyl chloride (Sigma-Aldrich, 97%), *p*-toluenesulfonyl chloride (ABCR, 98%), *N,N,N',N''*-pentamethyldiethyltriamine (PMDETA; Merck, 99.9%), 4-phenylazophenol (ABCR, 98%), potassium carbonate (VWR, rectapur), potassium iodide (Sigma-Aldrich, 99%), potassium phosphate monohydrate (Sigma-Aldrich, puriss.), propargyl alcohol (Alfa Aesar, 99%), silica gel (Merck, Geduran SI60. 0.063–0.200 mm), sodium acetate (Roth, 99%), sodium azide (Acros, 99%), sodium hydroxide (Roth, 99%), triethylamine (Acros, 99%), tetrabutylammonium hydrogen sulfate (Sigma-Aldrich, 97%), and triphenylphosphine (Merck, 99%) were used as received. Anhydrous dichloromethane (DCM) and tetrahydrofuran (THF) were purchased from Acros (extra dry over molecular sieves) and used as received. Diethyl ether (VWR Analpur) was dried over CaH<sub>2</sub> and distilled before use. Milli-Q water was obtained from a Milli-Q Advantage A10 Ultrapure Water Purification System (Millipore). All other solvents were of analytical grade and used as received. 2,2'-Azobis(2-methylpropionitrile) (AIBN; Fluka, 99%) was recrystallized twice from methanol. *N,N*-Diethylacrylamide (DEAAm; TCI, 98%) and *N,N*-dimethylacrylamide (DMAAm; TCI, 99%) were passed over a short column of basic alumina prior to use. *N*-(Adamantan-1-yl)-6-hydroxyhexanamide,<sup>19</sup> 2-(((2-carboxyethyl)thio)carbonothioyl)thio)-2-methylpropanoic acid (CEMP),<sup>43</sup> 2-(1-carboxy-1-methylethylsulfanylthiocarbonylsulfanyl)-2-methylpropionic acid (CMP),<sup>44</sup> 4-cyano-4-(((ethylthio)carbonothioyl)thio)pentanoate,<sup>45</sup> *N*-(2-hydroxypropyl)methacrylamide (HPMA),<sup>46</sup> mono-(6-azido-6-deoxy)- $\beta$ -CD ( $\beta$ -CD- $N_3$ ),<sup>47</sup> and 6-(4-(phenyldiazenyl)phenoxy)hexan-1-ol<sup>48</sup> were prepared according to the literature.

**Synthesis of 6-(Adamantan-1-ylamino)-6-oxohexyl-2-(((3-((6-(adamantan-1-ylamino)-6-oxohexyl)oxy)-3-oxopropyl)thio)carbonothioyl)thio)-2-methylpropanoate (CTA1).** Accord-

ing to a literature procedure,<sup>49</sup> CEMP (0.61 g, 2.26 mmol, 1.0 equiv), *N*-(adamantan-1-yl)-6-hydroxyhexanamide (1.50 g, 5.65 mmol, 2.5 equiv) and triphenylphosphine (1.48 g, 5.65 mmol, 2.5 equiv) were dissolved in dry THF (15 mL). At 0 °C DIAD (1.3 mL, 5.65 mmol, 2.5 equiv) in dry THF (5 mL) was added dropwise. The reaction mixture was stirred at ambient temperature overnight and subsequently for 3 h at 40 °C. After cooling to ambient temperature, DCM (50 mL) was added and the organic phase was washed twice with saturated NaHCO<sub>3</sub> solution (50 mL). The organic phase was dried over Na<sub>2</sub>SO<sub>4</sub> and filtered, and the solvent evaporated in vacuo. The residue was subjected to column chromatography on silica gel with *n*-hexane:ethyl acetate as eluent that was gradually changed from 1:1 to 1:2. The product was obtained as a yellow oil (0.88 g, 1.15 mmol, 51%). <sup>1</sup>H NMR (400 MHz, CDCl<sub>3</sub>): [δ, ppm] = 1.15–1.28 (m, 4H, 2 × CH<sub>2</sub>–CH<sub>2</sub>–CH<sub>2</sub>–C=O), 1.28–1.46 (m, 4H, 2 × CH<sub>2</sub>–CH<sub>2</sub>–O), 1.48–1.75 (m, 28H, 4 × (CH<sub>3</sub>)<sub>2</sub>–C, 2 × CH<sub>2</sub>–CH<sub>2</sub>–C=O; 6 × CH<sub>2</sub>,<sub>adamantyl</sub>), 1.92–2.01 (m, 12H, 6 × CH<sub>2</sub>,<sub>adamantyl</sub>–C–NH), 2.04–2.10 (m, 10H, 6 × CH<sub>2</sub>,<sub>adamantyl</sub>; 2 × CH<sub>2</sub>–C=O), 2.70 (t, 2H, CH<sub>2</sub>–CH<sub>2</sub>–S), 3.52 (t, 2H, CH<sub>2</sub>–S), 4.08 (q, 4H, 2 × CH<sub>2</sub>–O–C=O), 5.19 (br m, 2H, 2 × NH). <sup>13</sup>C NMR (100 MHz, CDCl<sub>3</sub>): [δ, ppm] = 25.5, 25.7, and 25.8 (2 × CH<sub>2</sub>–CH<sub>2</sub>–CH<sub>2</sub>–C=O; 2 × CH<sub>2</sub>–CH<sub>2</sub>–C=O, 2 × (CH<sub>3</sub>)<sub>2</sub>C), 28.3 and 28.5 (2 × CH<sub>2</sub>–CH<sub>2</sub>–O–C=O), 29.6 (6 × CH<sub>2</sub>,<sub>adamantyl</sub>), 31.4 (CH<sub>2</sub>–CH<sub>2</sub>–S), 33.2 (CH<sub>2</sub>–S), 36.5 (6 × CH<sub>2</sub>,<sub>adamantyl</sub>), 37.7 (2 × CH<sub>2</sub>–C=O), 41.9 (6 × CH<sub>2</sub>,<sub>adamantyl</sub>–C–NH), 51.9 (2 × C–NH), 56.4 (2 × C(CH<sub>3</sub>)<sub>2</sub>), 65.0 and 66.1 (2 × CH<sub>2</sub>–O–C=O), 171.5, 172.0, 172.1, and 172.9 (4 × C=O), 220.9 (C=S). ESI-MS: [M + Na<sup>+</sup>]<sub>exp</sub> = 785.58 *m/z* and [M + Na<sup>+</sup>]<sub>calc</sub> = 785.3668 *m/z*.

**Synthesis of Bis(6-(4-(phenyldiazanyl)phenoxy)hexyl)-2,2'-(thiocarbonylbis(sulfanediy))bis(2-methylpropanoate) (CTA2).** Based on a literature procedure,<sup>49</sup> CMP (1.00 g, 3.54 mmol, 1.0 equiv), 6-(4-(phenyldiazanyl)phenoxy)hexan-1-ol (3.38 g, 11.33 mmol, 3.2 equiv) and triphenylphosphine (2.97 g, 11.32 mmol, 3.2 equiv) were dissolved in dry THF (20 mL). At 0 °C DIAD (2.2 mL, 11.21 mmol, 3.2 equiv) in dry THF (20 mL) was added dropwise. The reaction mixture was stirred at ambient temperature overnight and subsequently for 3 h at 40 °C. After cooling to ambient temperature, DCM (100 mL) was added, and the organic phase was washed twice with saturated NaHCO<sub>3</sub> solution (100 mL). The organic phase was dried over Na<sub>2</sub>SO<sub>4</sub> and filtered, and the solvent evaporated in vacuo. The residue was subjected to column chromatography on silica gel with *n*-hexane:ethyl acetate as eluent that was gradually changed from 10:1 to 8:1. The product was obtained as an orange oil which solidified on cooling (2.77 g, 3.30 mmol, 93%). <sup>1</sup>H NMR (400 MHz, CDCl<sub>3</sub>): [δ, ppm] = 1.37–1.57 (m, 4H, 2 × CH<sub>2</sub>–CH<sub>2</sub>–CH<sub>2</sub>–O), 1.58–1.72 (m, 16H, 4 × C–CH<sub>3</sub>; 2 × O=C–O–CH<sub>2</sub>–CH<sub>2</sub>), 1.77–1.87 (m, 4H, 2 × O–CH<sub>2</sub>–CH<sub>2</sub>), 4.03 (t, 4H, 2 × CH<sub>2</sub>–O), 4.09 (t, 4H, 2 × CH<sub>2</sub>–O–C=O), 7.00 (d, 4H, 4 × CH<sub>arom</sub>), 7.40–7.46 (m, 2H, 2 × CH<sub>arom</sub>), 7.47–7.56 (m, 4H, 4 × C<sub>arom</sub>), 7.82–7.97 (m, 8H, 8 × CH<sub>arom</sub>). <sup>13</sup>C NMR (100 MHz, CDCl<sub>3</sub>): [δ, ppm] = 25.3 (4 × CH<sub>3</sub>–C), 25.8 and 25.9 (4 × CH<sub>2</sub>–CH<sub>2</sub>–CH<sub>2</sub>–O), 28.4 (2 × O–CH<sub>2</sub>–CH<sub>2</sub>), 29.2 (2 × O=C–O–CH<sub>2</sub>–CH<sub>2</sub>), 56.3 (2 × C(CH<sub>3</sub>)<sub>2</sub>), 66.1 (2 × O=C–O–CH<sub>2</sub>), 68.3 (2 × O–CH<sub>2</sub>), 114.8 (2 × O–C<sub>arom</sub>–CH<sub>arom</sub>), 122.7 (2 × CH<sub>arom</sub>), 124.9 (4 × CH<sub>arom</sub>), 129.2 (4 × CH<sub>arom</sub>), 130.4 (2 × CH<sub>arom</sub>), 147.0 (2 × C<sub>arom</sub>–N=N), 152.9 (2 × C<sub>arom</sub>–N=N), 161.8 (2 × O–C<sub>arom</sub>), 172.9 (2 × C=O), 218.6 (C=S). ESI-MS: [M + H<sup>+</sup>]<sub>exp</sub> = 843.33 *m/z* and [M + H<sup>+</sup>]<sub>calc</sub> = 843.3284 *m/z*.

**Synthesis of Prop-2-yn-1-yl-4-cyano-4-(((ethylthio)carbonothioyl)thio)pentanoate (CTA3).** In a 100 mL Schlenk flask, 4-cyano-4-(((ethylthio)carbonothioyl)thio)pentanoate (1.00 g, 3.80 mmol, 1.0 equiv), propargyl alcohol (0.5 mL, 8.65 mmol, 2.3 equiv), and DMAP (0.09 mg, 0.77 mmol, 0.2 equiv) were dissolved in anhydrous DCM (20 mL). At 0 °C a solution of DCC (1.57 g, 7.61 mmol, 2.0 equiv) in anhydrous DCM (10 mL) was added. After 1 h the solution was warmed to ambient temperature, stirred overnight, filtered, and concentrated under reduced pressure. The residue was purified via column chromatography on silica-gel with *n*-hexane:ethyl acetate 10:1 as eluent. The product was obtained as a yellow oil (0.94 g, 3.13 mmol, 82%). <sup>1</sup>H NMR (400 MHz, CDCl<sub>3</sub>): [δ, ppm] = 1.35 (t, 3H, *J* = 7.4 Hz, CH<sub>2</sub>–CH<sub>3</sub>), 1.87 (s, 3H, C–CH<sub>3</sub>), 2.27–2.59 (m, 3H,

CH, CH<sub>2</sub>–COO), 2.62–2.76 (m, 2H, C–CH<sub>2</sub>), 3.34 (q, 2H, *J* = 7.4 Hz, CH<sub>3</sub>–CH<sub>2</sub>), 4.71 (d, 2H, CH<sub>2</sub>–C–CH). <sup>13</sup>C NMR (100 MHz, CDCl<sub>3</sub>): [δ, ppm] = 12.9 (CH<sub>3</sub>), 25.0 (C–CH<sub>3</sub>), 29.7 (CH<sub>2</sub>–COO), 31.5 (C–CH<sub>2</sub>), 33.8 (CH<sub>3</sub>–CH<sub>2</sub>), 46.4 (C–CH<sub>2</sub>), 52.6 (CH<sub>2</sub>–C–CH), 75.4 (CH<sub>2</sub>–C–CH), 77.4 (CH<sub>2</sub>–C–CH), 119.0 (C–N), 170.8 (C=O), 216.8 (C=S). ESI-MS: [M + Na<sup>+</sup>]<sub>exp</sub> = 324.08 *m/z* and [M + Na<sup>+</sup>]<sub>calc</sub> = 324.0163 *m/z*.

**Exemplary Procedure for the RAFT Polymerization of DEAAm.** CTA1 (54.9 mg, 0.07 mmol, 1.0 equiv), DEAAm (500.0 mg, 3.94 mmol, 56.3 equiv), AIBN (4.2 mg, 0.03 mmol, 0.4 equiv), DMF (3.3 mL), and a stirring bar were added into a Schlenk tube. After three freeze–pump–thaw cycles the tube was backfilled with argon, sealed, placed into an oil bath at 60 °C, and removed after 24 h. The tube was subsequently cooled with liquid nitrogen to stop the reaction. An NMR sample was withdrawn for the determination of conversion, inhibited with a pinch of hydroquinone (~5 mg), and CDCl<sub>3</sub> was added. Quantitative conversion was estimated based on the NMR data (see the Characterization and Methods section for details of the calculation). The residue was dialyzed against deionized water with a SpectraPor3 membrane (MWCO = 1000 Da) for 3 days at ambient temperature. The solvent was removed in vacuo to yield the polymer as a yellow solid (422.0 mg, 76%, GPC (THF): *M*<sub>n,GPC</sub> = 6500 g mol<sup>-1</sup>, *D*<sub>M</sub> = 1.11).

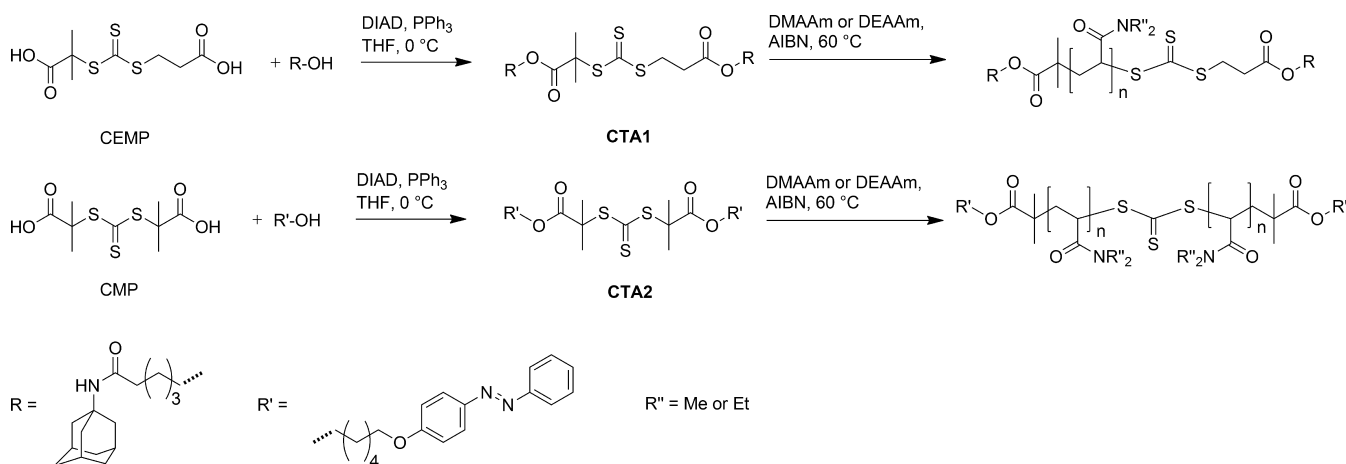
**Exemplary Procedure for the RAFT Polymerization of HPMA.** CTA3 (60.5 mg, 0.20 mmol, 1.0 equiv), HPMA (2.00 g, 14.18 mmol, 35.5 equiv), V-501 (11.6 mg, 0.04 mmol, 0.2 equiv), DMF (6.0 mL), acetic acid/sodium acetate buffer (pH 5.2, 0.27 M acetic acid and 0.73 M sodium acetate; 6.0 mL), and a stirring bar were added into a Schlenk tube. After three freeze–pump–thaw cycles the tube was backfilled with argon, sealed, placed into an oil bath at 70 °C, and removed after 2 h. The tube was subsequently cooled with liquid nitrogen to stop the reaction. A NMR sample was withdrawn for the determination of conversion, inhibited with a pinch of hydroquinone (~5 mg), and D<sub>2</sub>O was added. A conversion of 23% was estimated based on the NMR data (see the Characterization and Methods section for details of the calculation). The residue was dialyzed against deionized water with a SpectraPor3 membrane (MWCO = 1000 Da) for 3 days at ambient temperature. The solvent was removed in vacuo to yield the polymer as a yellow solid (0.37 g, 80%, GPC (DMAc): *M*<sub>n,GPC</sub> = 6500 g mol<sup>-1</sup>, *D*<sub>M</sub> = 1.17).

**Exemplary Click Reaction of Alkyne-Functionalized PHPMA with β-CD-N<sub>3</sub>.** Alkyne-functionalized PHPMA (*M*<sub>n,GPC</sub> = 6500 g mol<sup>-1</sup>; 150.0 mg, 0.023 mmol, 1.0 equiv), β-CD-N<sub>3</sub> (133.8 mg, 0.115 mmol, 5.0 equiv), PMDETA (34 μL, 0.163 mmol, 7.1 equiv), DMF (5.3 mL), and a stirring bar were introduced into a Schlenk tube. After three freeze–pump–thaw cycles the tube was filled with argon, and CuBr (19.8 mg, 0.138 mmol, 6.0 equiv) was added under a stream of argon. Subsequently, two freeze–pump–thaw cycles were performed, the tube was backfilled with argon, and the mixture was stirred at ambient temperature for 24 h. EDTA solution (5 wt %, 1 mL) was added, and the residue was dialyzed against deionized water with a SpectraPor3 membrane (MWCO = 2000 Da) for 3 days at ambient temperature. The solvent was removed in vacuo to yield the CD-functionalized polymer as a yellow solid (96.0 mg, 55%, GPC (DMAc): *M*<sub>n,GPC</sub> = 7300 g mol<sup>-1</sup>, *D*<sub>M</sub> = 1.29).

**Exemplary Supramolecular ABA Block Copolymer Formation via Cyclodextrin/Guest Interaction.** CD-functionalized PHPMA (*M*<sub>n,GPC</sub> = 7300 g mol<sup>-1</sup>; 70.0 mg, 0.0096 mmol, 2.0 equiv) was dissolved in DMF (4 mL) and added dropwise to a solution of doubly adamantyl-functionalized PDMAAm (*M*<sub>n,GPC</sub> = 6400 g mol<sup>-1</sup>; 30.0 mg, 0.0047 mmol, 1.0 equiv) in DMF (2 mL) under vigorous stirring. The resulting solution was dialyzed against a deionized water/DMF mixture with a SpectraPor3 (MWCO = 1000 Da) membrane at 4 °C. The water content was gradually changed from 70% to 100% over 1 day, and the dialysis was continued for 3 days with deionized water at 4 °C. The solvent was removed in vacuo to yield the supramolecular complex in quantitative yield.

**Characterization and Methods.** NMR measurements were carried out on a Bruker AM250 spectrometer at 250 MHz for hydrogen nuclei for conversion determination and a Bruker AM400

## Scheme 2. Overview of the Synthetic Pathway Leading to the Doubly Guest-Functionalized Inner Building Block Featuring Adamantyl or Azobenzene Guest Groups



spectrometer at 400 MHz for hydrogen nuclei and at 100 MHz for carbon nuclei for structure verification. 2D NOESY (nuclear Overhauser effect spectroscopy) spectra were measured on a Bruker Avance III 600 spectrometer at 600 MHz with a mixing time of 0.3 s and a concentration of 60 mg mL<sup>-1</sup>. For the determination of the conversion of DMAAm the integrals of one vinylic proton (5.78–5.89 ppm) and the backbone protons (0.75–2.00 ppm) were employed. The conversion of DEAAm was determined with the integral of one vinylic proton (5.57–5.73 ppm) and with the integral of the side chain methyl groups and backbone protons (0.81–1.97 ppm). The conversion of HPMA was calculated with the integral of one vinylic proton (5.48–5.58 ppm) and with the integral of one side-chain proton (3.86–4.14).

Size exclusion chromatography (SEC) with *N,N*-dimethylacetamide (DMAc) as eluent containing 0.03 wt % LiBr was performed for PDMAAm and PHPMA on a Polymer Laboratories PL-GPC 50 Plus Integrated System, comprising an autosampler, a PLgel 5  $\mu\text{m}$  bead-size guard column (50  $\times$  7.5 mm) followed by three PLgel 5  $\mu\text{m}$  MixedC columns (300  $\times$  7.5 mm), and a differential refractive index detector at 50  $^\circ\text{C}$  with a flow rate of 1.0 mL min<sup>-1</sup>. The SEC system was calibrated against linear poly(styrene) standards with molecular weights ranging from 160 to 6  $\times$  10<sup>6</sup> g mol<sup>-1</sup> or poly(methyl methacrylate) standards with molecular weights ranging from 700 to 2  $\times$  10<sup>6</sup> g mol<sup>-1</sup>. All SEC calculations for PDMAAm were carried out relative to a poly(styrene) calibration. The SEC calculations for PHPMA were carried out relative to a poly(methyl methacrylate) calibration. SEC with tetrahydrofuran (THF) as eluent containing 200 ppm 2,6-di-*tert*-butyl-4-methylphenol for PDEAAm was performed on a Polymer Laboratories PL-GPC 50 Plus Integrated System, comprising an autosampler, a PLgel 5  $\mu\text{m}$  bead-size guard column (50  $\times$  7.5 mm) followed by three PLgel 5  $\mu\text{m}$  MixedC columns (300  $\times$  7.5 mm), a PLgel 5  $\mu\text{m}$  MixedE column (300  $\times$  7.5 mm), and a differential refractive index detector at 35  $^\circ\text{C}$  with a flow rate of 1.0 mL min<sup>-1</sup>. The SEC system was calibrated against linear poly(styrene) standards with molecular weights ranging from 160 to 6  $\times$  10<sup>6</sup> g mol<sup>-1</sup>. All SEC calculations for PDEAAm were carried out relative to poly(styrene) calibration. The molecular weight dispersity is abbreviated as  $D_M$ .

Electrospray ionization–mass spectrometry (ESI-MS) was performed on an LXQ mass spectrometer (ThermoFisher Scientific, San Jose, CA) equipped with an atmospheric pressure ionization source operating in the nebulizer-assisted electrospray mode. The instrument was calibrated in the  $m/z$  range 195–1822 Da using a standard containing caffeine, Met-Arg-Phe-Ala acetate (MRFA), and a mixture of fluorinated phosphazenes (Ultramark 1621) (all from Aldrich). A constant spray voltage of 4.5 kV was used, and nitrogen at a dimensionless sweep gas flow rate of 2 ( $\sim$ 3 L min<sup>-1</sup>) and a dimensionless sheath gas flow rate of 12 ( $\sim$ 1 L min<sup>-1</sup>) were applied.

The capillary voltage, the tube lens offset voltage, and the capillary temperature were set to 60 V, 110 V, and 275  $^\circ\text{C}$ , respectively.

Cloud points were measured on a Cary 300 Bio UV/vis spectrophotometer (Varian) at 600 nm. The heating rate was set to 0.32  $^\circ\text{C min}^{-1}$  and the concentration at 1 mg mL<sup>-1</sup>. For the determination of the cloud point the point of inflection of the transmittance vs temperature plot was used.

Dynamic light scattering (DLS) was performed on a 380 DLS spectrometer (Particle Sizing Systems, Santa Barbara, CA) with a 90 mW laser diode operating at 658 nm equipped with an avalanche photodiode detector. Every measurement was performed four times at 10  $^\circ\text{C}$  for samples containing PDEAAm and at 25  $^\circ\text{C}$  for samples containing PDMAAm. The data was evaluated with an inverse Laplace algorithm. The scattered light was recorded at an angle of 90 $^\circ$  to the incident beam. For the temperature sequenced measurements the sample was equilibrated at the specific temperature for 5 min, then the DLS measurement was performed 3 times for 3 min, and the temperature was changed again. The entire procedure was performed three times, and the data points were finally averaged. All hydrodynamic diameters ( $D_h$ ) in the text are the averages of the number-weighted distributions. The samples were prepared in Milli-Q water and filtered with a 0.2  $\mu\text{m}$  regenerated cellulose syringe filter (Roth, Rotilabo).

UV/vis spectra were measured on a Cary 300 Bio UV/vis spectrophotometer (Varian) at a temperature of 25 or 10  $^\circ\text{C}$  depending on the sample.

UV irradiation for investigation of photoresponse was applied via a BLB-8 UV lamp (8 W, Camag) with an emission maximum at 350 nm (refer to Figure S36 for the emission spectrum) for the DLS samples and via a UVASPOT 2000RF2 (2000 W, Hönle technology) with its main irradiation between 315 and 420 nm for the NMR samples.

Theoretical molecular weights were calculated with the equation

$$M_{\text{theo}} = \text{conversion} \times M(\text{monomer}) \times \frac{[\text{monomer}]_0}{[\text{CTA}]_0} + M(\text{CTA})$$

## RESULTS AND DISCUSSION

**Synthesis of the Building Blocks.** For the synthesis of the inner building blocks two doubly guest-functionalized CTAs based on trithiocarbonates were designed. CTA1 contains two adamantyl groups, and CTA2 contains two azobenzene groups. The adamantyl group was chosen due to its high complexation constant of up to 10<sup>5</sup> M<sup>-1</sup> with  $\beta$ -CD.<sup>50</sup> The azobenzene group was chosen due its ability to change the conformation from *trans* to *cis* in response to light irradiation. This change in conformation leads to a significant change in the complexation constant with  $\beta$ -CD; i.e., the guest is expelled from the host

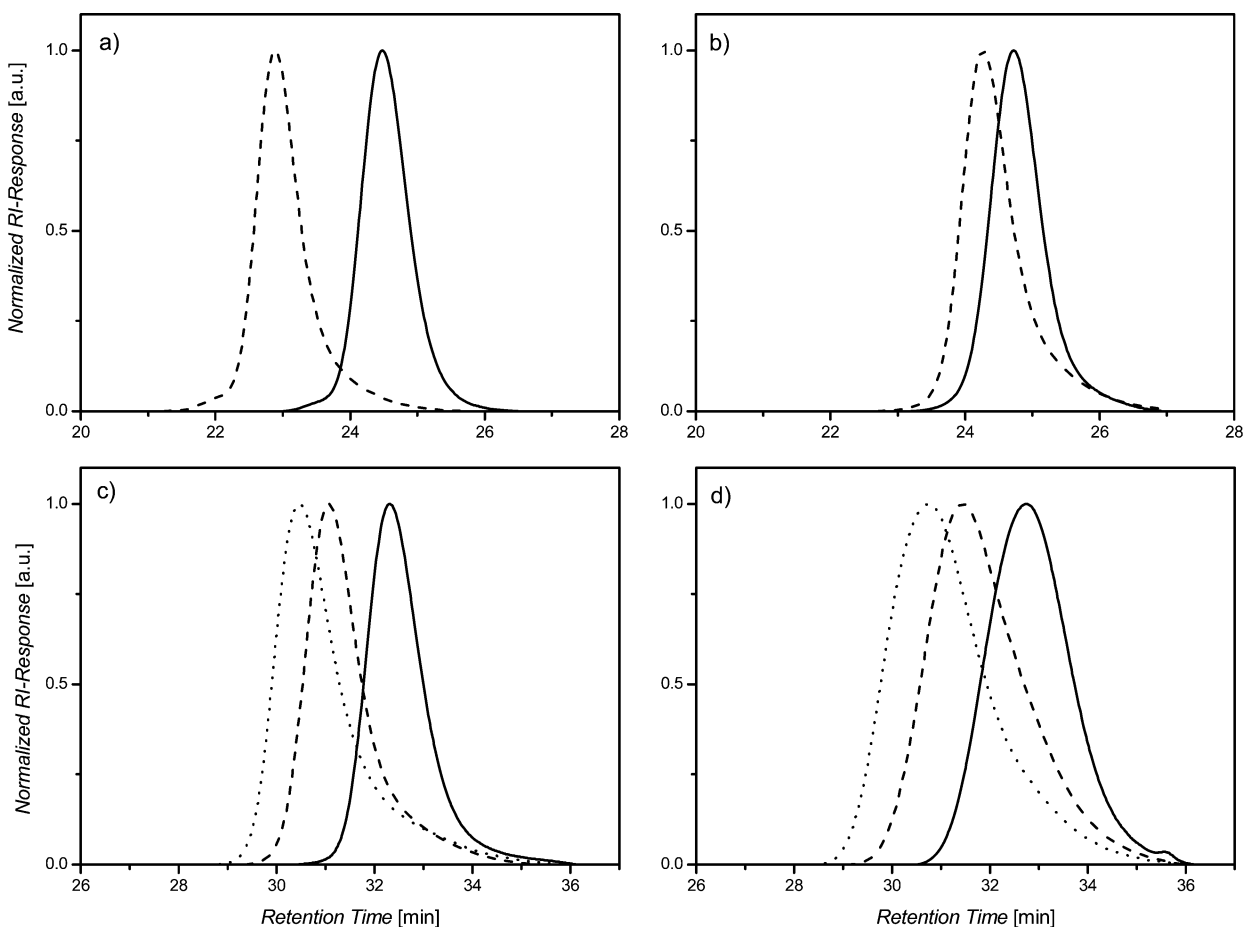
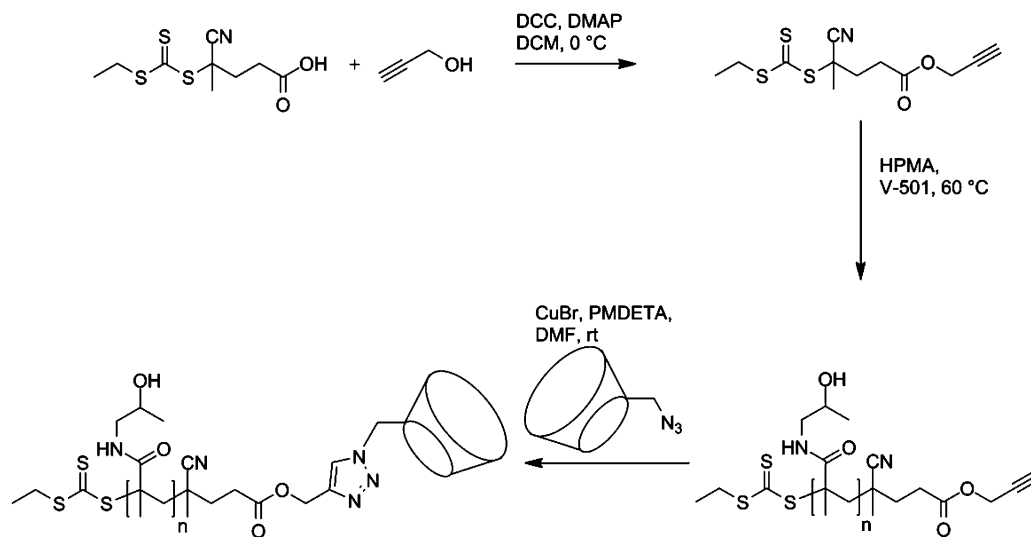


**Figure 1.** SEC traces for (a) PDMAAm polymerized with CTA1 (dashed line: PDMAAm<sub>151</sub>-Ad<sub>2</sub>; solid line: PDMAAm<sub>57</sub>-Ad<sub>2</sub>), (b) PDMAAm polymerized with CTA2 (dashed line: PDMAAm<sub>103</sub>-Azo<sub>2</sub>; solid line: PDMAAm<sub>46</sub>-Azo<sub>2</sub>), (c) PDEAAm polymerized with CTA1 (dotted line: PDEAAm<sub>89</sub>-Ad<sub>2</sub>; dashed line: PDEAAm<sub>78</sub>-Ad<sub>2</sub>; solid line: PDEAAm<sub>45</sub>-Ad<sub>2</sub>), and (d) PDEAAm polymerized with CTA2 (dotted line: PDEAAm<sub>80</sub>-Azo<sub>2</sub>; dashed line: PDEAAm<sub>59</sub>-Azo<sub>2</sub>; solid line: PDEAAm<sub>36</sub>-Azo<sub>2</sub>).

### Scheme 3. Overview of the Synthetic Pathway Leading to the $\beta$ -CD-Functionalized Outer PHPMA Building Block



molecule upon irradiation with UV light. The guest molecules were attached to the core CTA molecule via a short spacer group to support its availability in the complex formation. As shown in Scheme 2, both guest-functionalized CTAs were synthesized via a Mitsunobu reaction from the corresponding

acids: CEMP in the case of CTA1 and CMP in the case of CTA2.

Subsequently, the novel CTAs were employed in the RAFT polymerization of DMAAm and DEAAm in DMF at 60 °C with AIBN as initiator. DMAAm was selected to investigate the

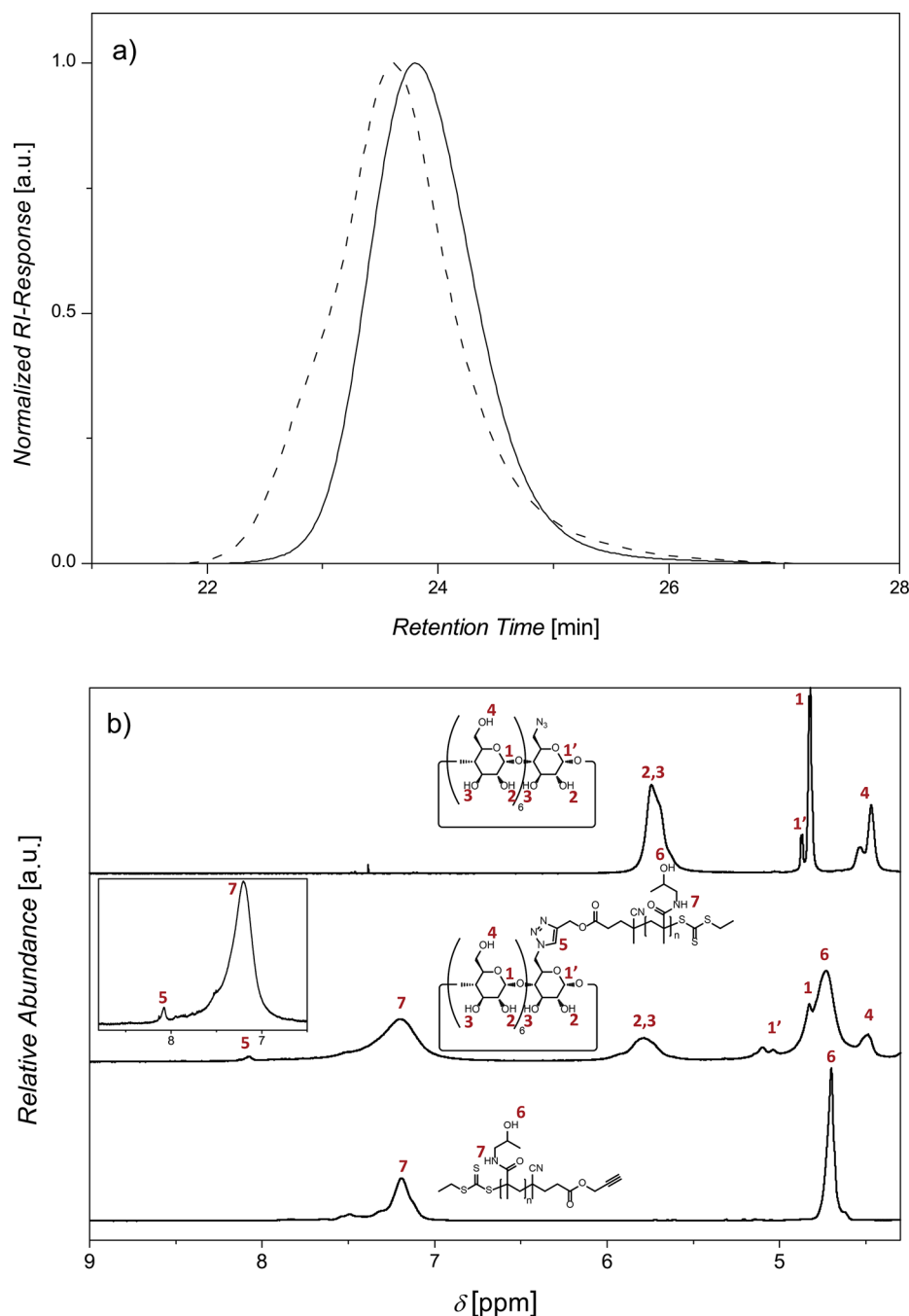


**Figure 2.** (a) SEC traces for PHPMA polymerized with CTA3 (solid line: PHPMA<sub>44</sub>-alkyne) and the product of the conjugation with β-CD-N<sub>3</sub> (dashed line: PHPMA<sub>44</sub>-β-CD) and (b) comparison of the <sup>1</sup>H NMR spectra of β-CD-N<sub>3</sub> (top), the β-CD-functionalized PHPMA click product (middle: PHPMA<sub>28</sub>-β-CD), and alkyne-functionalized PHPMA (bottom: PHPMA<sub>28</sub>-alkyne).

temperature response of the complex formation whereas DEAAm was chosen due to its cloud point, providing the opportunity to study the formation of block copolymer aggregates in solution due to a coil-to-globule transition of PDEAAm above the cloud point. In the case of PDMAAm, molecular weights of 6400 and 15 700 g mol<sup>-1</sup> with a  $\mathcal{D}_M$  (molecular-weight dispersity) of 1.06 and 1.11, respectively, were achieved with CTA1, while a molecular weight of 5400 and 11 000 g mol<sup>-1</sup> with a  $\mathcal{D}_M$  of 1.08 and 1.11, respectively, were reached with CTA2 (refer to Figure 1a,b, Figures S9 and S10, and Table S1). The polymerization of DEAAm with CTA1 afforded polymers with molecular weights ranging from

6500 to 12 100 g mol<sup>-1</sup> and  $\mathcal{D}_M$  ranging from 1.11 to 1.27 (refer to Figure 1c, Figure S11, and Table S2). Furthermore, PDEAAms with molecular weights ranging from 5400 to 11 000 g mol<sup>-1</sup> and  $\mathcal{D}_M$  ranging from 1.16 to 1.33 (refer to Figure 1d, Figure S12, and Table S3) were synthesized with CTA2. The structure of the polymers was verified via <sup>1</sup>H NMR and ESI-MS (refer to Figures S13–S20).

For the outer building block the biocompatible monomer HPMA was utilized.<sup>41</sup> Therefore, a trithiocarbonate CTA with an alkyne moiety was synthesized (refer to Scheme 3). A dithiobenzoate CTA, the first choice for methacrylamide and methacrylate monomers, was not further considered as the

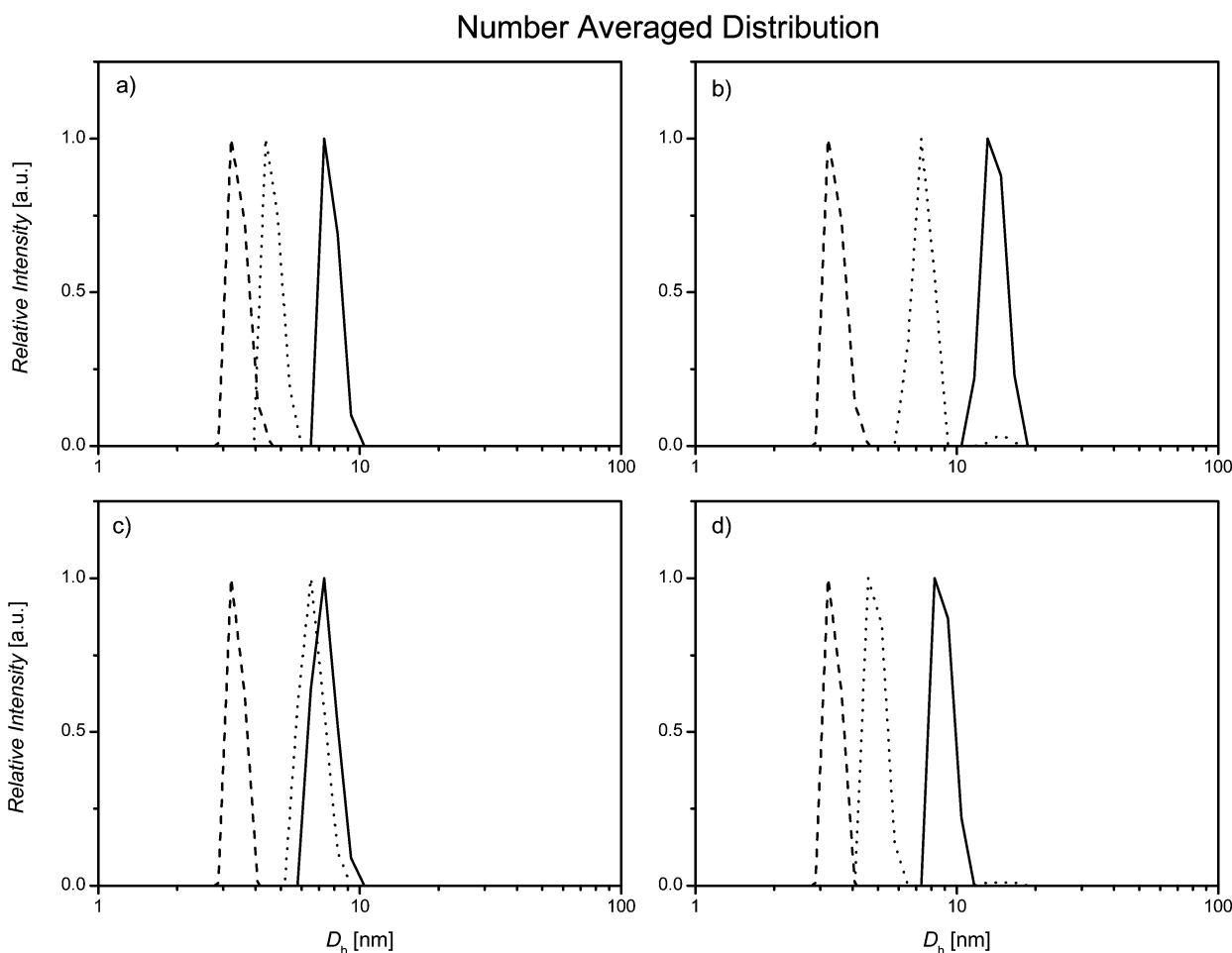


**Figure 3.** Comparison of the number-averaged particle size distributions of the building blocks (dashed line: PHPMA; dotted line: PDMAAM or PDEAAM) and the supramolecular block copolymer (solid line) at a concentration of 1 mg mL<sup>-1</sup>: (a) PHPMA<sub>26</sub>- $\beta$ -CD, PDMAAM<sub>151</sub>-Ad<sub>2</sub> and PDMAAM<sub>151</sub>-Ad<sub>2</sub>-*b*-(PHPMA<sub>26</sub>- $\beta$ -CD)<sub>2</sub> at 25 °C; (b) PHPMA<sub>26</sub>- $\beta$ -CD, PDMAAM<sub>103</sub>-Azo<sub>2</sub>, and PDMAAM<sub>103</sub>Azo<sub>2</sub>-*b*-(PHPMA<sub>26</sub>- $\beta$ -CD)<sub>2</sub> at 25 °C; (c) PHPMA<sub>28</sub>- $\beta$ -CD, PDEAAM<sub>89</sub>-Ad<sub>2</sub>, and PDEAAM<sub>89</sub>-Ad<sub>2</sub>-*b*-(PHPMA<sub>28</sub>- $\beta$ -CD)<sub>2</sub> at 10 °C; (d) PHPMA<sub>28</sub>- $\beta$ -CD and PDEAAM<sub>80</sub>-Azo<sub>2</sub>-*b*-(PHPMA<sub>28</sub>- $\beta$ -CD)<sub>2</sub> at 10 °C.

complex formation between the phenyl group and  $\beta$ -CD cannot be ruled out. As the utilized CTA contains an unprotected alkyne moiety, the conversion in the RAFT polymerizations was kept at low values to suppress radical transfer to the terminal alkyne.

The polymerization of HPMA was conducted in a mixture of DMF and acetic acid/sodium acetate buffer with V-501 as initiator at 70 °C. The utilization of CTA3 afforded narrowly distributed alkyne-functionalized PHPMA, e.g., a molecular weight of 6500 g mol<sup>-1</sup> and a  $\bar{D}_M$  of 1.17 (refer to Figure 2, Figures S21 and S22, and Table S8). The structure of the polymer was proven via ESI-MS and <sup>1</sup>H NMR measurements (refer to Figures S23 and S24). The subsequent functionalization with  $\beta$ -CD was accomplished via a CuAAC reaction of the alkyne-functionalized PHPMA and  $\beta$ -CD-N<sub>3</sub>. In the SEC trace a shift of the RI signal to lower retention times is evident, thus proving the increased hydrodynamic volume of the  $\beta$ -CD conjugated PHPMA in comparison with the alkyne-functionalized PHPMA (refer to Figure 2a and Figure S25). Furthermore, the  $M_n$  of the molecular weight distribution increases from 6500 to 7300 g mol<sup>-1</sup>. The distribution has a small shoulder at higher molecular weights that could be due to the conjugation of small amounts of difunctional azido  $\beta$ -CD. In other cases with lower molecular weight PHPMA (refer to

Table S10), the  $M_n$  of the distribution remains close to unchanged. Nevertheless, the peak maximum molecular weight ( $M_p$ ) increases as expected (Table S10), and a shift of the distribution is visible.

Furthermore, <sup>1</sup>H NMR shows the formation of the triazole ring as the new signal at 8.1 ppm can be assigned to the triazole proton (Figure 2b inset). Additionally, the <sup>1</sup>H NMR spectrum shows signals that can be assigned to both  $\beta$ -CD and PHPMA, e.g., the anomeric CD protons between 4.3 and 4.6 ppm, the 2-hydroxyl and the 3-hydroxyl protons between 5.5 and 6.0 ppm, the hydroxyl protons of PHPMA between 4.6 and 4.8 ppm, or the amide proton of PHPMA between 7.0 and 7.5 ppm (see Figure 2b).

**Self-Assembly of the Building Blocks to Form ABA Triblock Copolymers.** To ensure the availability of the hydrophobic guest groups for the complex formation, the self-assembly of the building blocks was accomplished via the dialysis method. In brief, both polymer building blocks were dissolved in an organic solvent, e.g., DMF, one solution was added dropwise to the other under vigorous stirring, and the organic solvent was removed via dialysis. The complexes were finally lyophilized and subsequently characterized via DLS and NOESY-NMR.

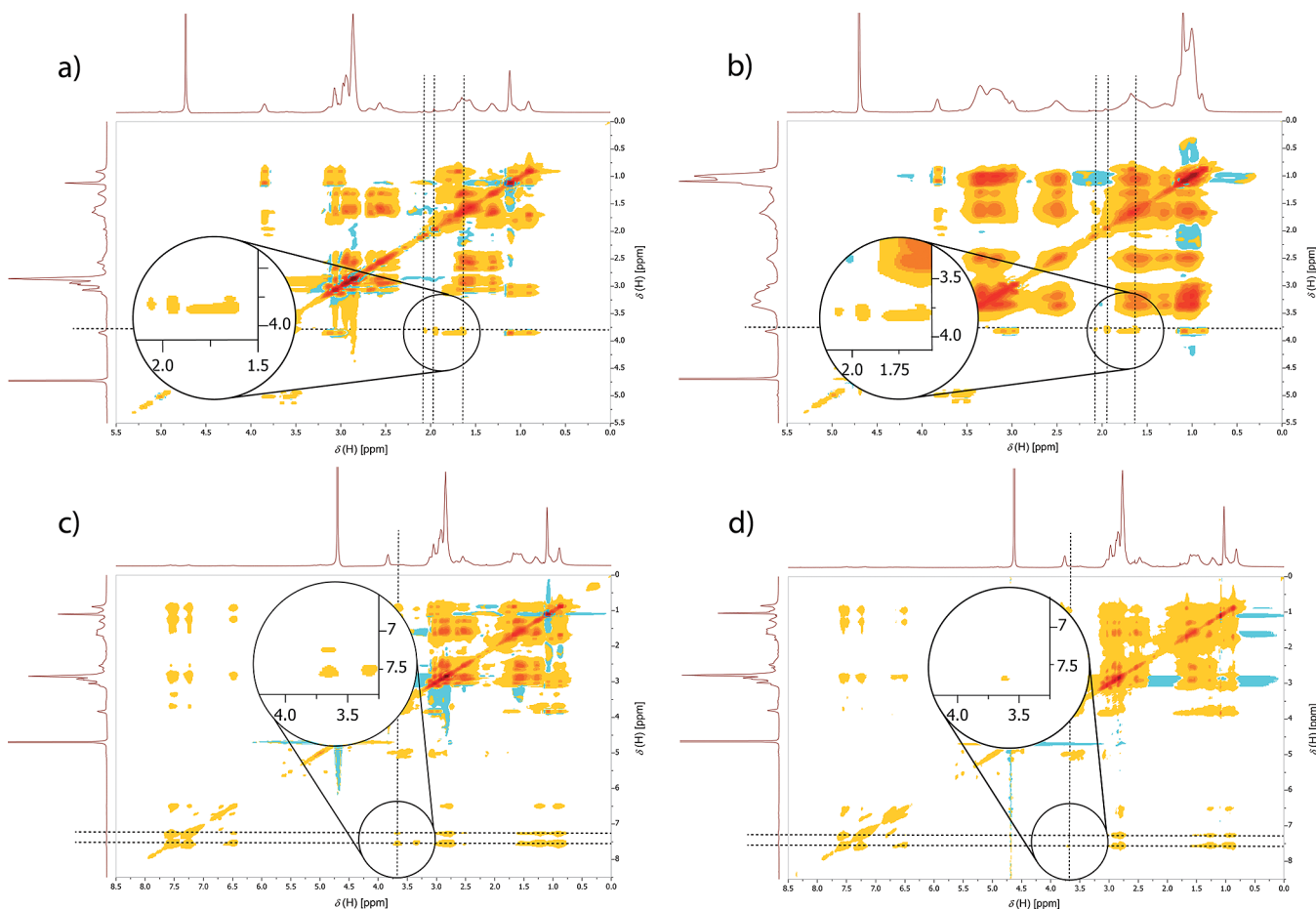


**Figure 4.** 2D NOESY NMR spectra of the supramolecular triblock copolymers in  $D_2O$  at 25 °C: (a) PDMAAm<sub>151</sub>Ad<sub>2</sub>-*b*-(PHPMA<sub>26</sub>- $\beta$ -CD)<sub>2</sub>; (b) PDEAAm<sub>78</sub>Ad<sub>2</sub>-*b*-(PHPMA<sub>28</sub>- $\beta$ -CD)<sub>2</sub>; (c) PDMAAm<sub>103</sub>Azo<sub>2</sub>-*b*-(PHPMA<sub>26</sub>- $\beta$ -CD)<sub>2</sub>; (d) PDMAAm<sub>103</sub>Azo<sub>2</sub>-*b*-(PHPMA<sub>26</sub>- $\beta$ -CD)<sub>2</sub> after UV irradiation for 7 min.

DLS is a versatile tool to investigate the complex formation in solution. In our investigation we employed DLS to obtain the hydrodynamic diameter ( $D_h$ ) of the polymer coils in solution. In principle, the  $D_h$  should increase upon complex formation as three polymer chains are included in the complex. The PDMAAm based complexes were measured at 25 °C, and the complexes show larger  $D_h$  than the individual parts (refer to Figure 3, Figure S26, and Table S11); e.g., PHPMA<sub>26</sub>- $\beta$ -CD has a  $D_h$  of 3.4 nm, PDMAAm<sub>151</sub>-Ad<sub>2</sub> has a  $D_h$  of 4.7 nm, and the supramolecular complex features a  $D_h$  of 7.8 nm. An exception is the doubly adamantyl-functionalized PDMAAm with lower molecular weight, which has a  $D_h$  of 175.0 nm for PDMAAm<sub>57</sub>-Ad<sub>2</sub>, a  $D_h$  of 5.1 for PHPMA<sub>44</sub>- $\beta$ -CD, and a  $D_h$  of 15.4 nm for the supramolecular complex PDMAAm<sub>57</sub>-Ad<sub>2</sub>-*b*-(PHPMA<sub>44</sub>- $\beta$ -CD)<sub>2</sub>. In this case, the hydrophobic guest groups lead to aggregation of or within the homopolymer. The complex shows a smaller  $D_h$ , yet the value of 15.4 nm suggests further aggregation probably due to more complicated structures in solution. An example for doubly azobenzene-functionalized PDMAAm is PDEAAm<sub>80</sub>Azo<sub>2</sub>-*b*-(PHPMA<sub>28</sub>- $\beta$ -CD)<sub>2</sub> with a  $D_h$  of 8.9 nm. The individual building blocks PDEAAm<sub>80</sub>Azo<sub>2</sub> and PHPMA<sub>28</sub>- $\beta$ -CD have a  $D_h$  of 4.9 and 3.4 nm, respectively.

Because of the cloud point of PDEAAm the DLS measurements were performed at 10 °C in that case. A significant increase in  $D_h$  was evident in most of the cases (refer to Figure 3, Figure S26, and Table S11). An example for doubly adamantyl-functionalized PDEAAm is PDEAAm<sub>89</sub>-Ad<sub>2</sub>-*b*-

(PHPMA<sub>28</sub>- $\beta$ -CD)<sub>2</sub> with a  $D_h$  of 7.4 nm consisting of PDEAAm<sub>89</sub>-Ad<sub>2</sub> with a  $D_h$  of 6.6 nm and PHPMA<sub>28</sub>- $\beta$ -CD with a  $D_h$  of 3.4 nm. Similar to PDMAAm lower molecular weight, doubly adamantyl-functionalized PDEAAm shows very large  $D_h$  (48.4 nm for PDEAAm<sub>45</sub>-Ad<sub>2</sub>) for the homopolymer and a  $D_h$  of 6.1 nm after complexation with PHPMA<sub>28</sub>- $\beta$ -CD. For doubly azobenzene-functionalized PDEAAm an increase in  $D_h$  from 4.9 nm for the middle-block PDEAAm<sub>80</sub>-Azo<sub>2</sub> and 3.4 nm for the outer PHPMA<sub>28</sub>- $\beta$ -CD blocks to 8.9 nm is observed for the complex.

To evidence the molecular nature of the complex formation NOESY NMR was utilized which is a well-suited tool to study host/guest complex formation. The adamantyl-based systems PDMAAm<sub>151</sub>Ad<sub>2</sub>-*b*-(PHPMA<sub>26</sub>- $\beta$ -CD)<sub>2</sub> and PDEAAm<sub>78</sub>Ad<sub>2</sub>-*b*-(PHPMA<sub>28</sub>- $\beta$ -CD)<sub>2</sub> show cross-correlation peaks that correspond to the signals of the adamantyl moiety at 1.72, 2.04, and 2.16 ppm and the inner protons of  $\beta$ -CD between 3.5 and 3.8 ppm (Figure 4a,b). This proves the close spatial proximity of the adamantyl moiety and the inner CD protons which is the case for inclusion complexes. NOESY spectra of the azobenzene-based systems show weak cross-correlation peaks originating from the azobenzene protons between 7.0 and 7.5 ppm and the inner CD protons (refer to Figure 4c and Figure S27). The azobenzene moiety shows weaker cross-correlation peaks in comparison with adamantyl systems which can be explained with the weaker complexation and the larger distance between the CD protons and the aromatic protons in the

## Number Averaged Distribution

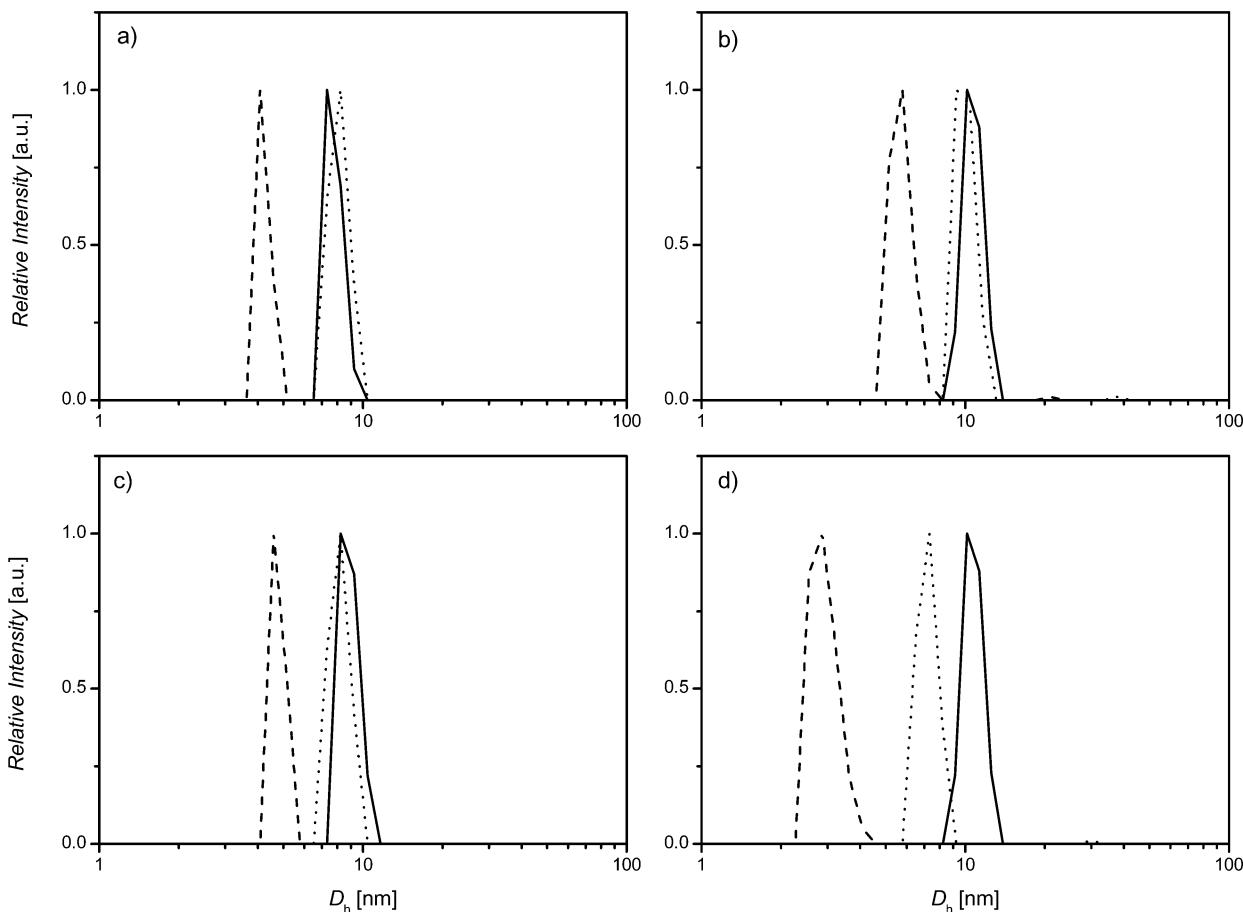


**Figure 5.** Number-averaged particle size distributions before applying the stimulus (solid line), during or directly after applying the stimulus (dashed line) and after standing at ambient temperature/in daylight for the specified time (dotted line): (a) complex PDMAAm<sub>151</sub>Ad<sub>2</sub>-b-(PHPMA<sub>26</sub>-β-CD)<sub>2</sub> before heating, during heating to 70 °C and after 3 days; (b) complex PDMAAm<sub>103</sub>Azo<sub>2</sub>-b-(PHPMA<sub>26</sub>-β-CD)<sub>2</sub> before heating, during heating to 70 °C and after 1 day; (c) complex PDEAAm<sub>80</sub>Azo<sub>2</sub>-b-(PHPMA<sub>28</sub>-β-CD)<sub>2</sub> before irradiation, directly after irradiation at 350 nm for 30 min and after 2 days; (d) complex PDMAAm<sub>103</sub>Azo<sub>2</sub>-b-(PHPMA<sub>26</sub>-β-CD)<sub>2</sub> before irradiation, directly after irradiation at 350 nm for 30 min and after 1 day.

azobenzene. Nevertheless, the spectra are a strong hint for inclusion complex formation. In general, the observed cross-correlation peaks are weaker in the case of PDEAAm containing samples as the concentration of the NMR samples was lower due to less solubility of the block copolymer in D<sub>2</sub>O compared to the PDMAAm-based copolymers.

In general, the described supramolecular ABA block copolymer is in equilibrium with the building blocks due to its noncovalent nature. Therefore, the existence of AB block copolymers and nonconnected building blocks cannot be excluded. However, the formation of the desired structure is governed by the equilibrium constants that are rather high in the described systems. Thus, the ABA block copolymer should be present almost exclusively in solution.

**Investigations of the Stimuli-Responsive Behavior of the Supramolecular Assemblies.** The prepared CD-based host/guest complexes show thermoresponsivity due to the usually negative enthalpy of complex formation.<sup>19,51,52</sup> To evidence the thermoresponsivity of the host/guest supramolecular triblock copolymers, guest-functionalized PDMAAm was synthesized that features no cloud point. As shown in Figure 5a,b, both the adamantyl- and azobenzene-based triblock copolymers show a significant decrease in  $D_h$  from 7.8 to 4.2 nm for an adamantyl guest in the case of PDMAAm<sub>151</sub>Ad<sub>2</sub>-b-

(PHPMA<sub>26</sub>-β-CD)<sub>2</sub> and from 11.2 to 5.4 nm in the case of azobenzene in PDMAAm<sub>103</sub>Azo<sub>2</sub>-b-(PHPMA<sub>26</sub>-β-CD)<sub>2</sub> upon heating to 70 °C (additional examples are listed in the Supporting Information, Figure S28 and Table S12). Furthermore, the complexes form again after remaining at ambient temperature which is proven by an increase in  $D_h$  close to the original values. In the case of lower molecular weight PDMAAm, the  $D_h$  increases with heating which is due to the formation of aggregates in solution as the complex dissociates. These aggregates could be formed due to the hydrophobic guest groups that are unmasked which changes the solubility of the PDMAAm. In analogy to the higher molecular weight PDMAAm, the complexes reform again after remaining at ambient temperature for 3–4 days and the  $D_h$  decreases. The rate of the re-formation of the complexes can be followed by DLS. It seems that azobenzene-based complexes form faster, which may be attributed to the increased polarity of azobenzene compared to adamantane which enhances the accessibility of the guest moiety in aqueous solution. Moreover, the re-formation of the complexes is faster with a higher degree of polymerization of PDMAAm. An explanation for that effect is the overall solubility of the polymer chain that changes drastically after the complex dissociation for lower molecular

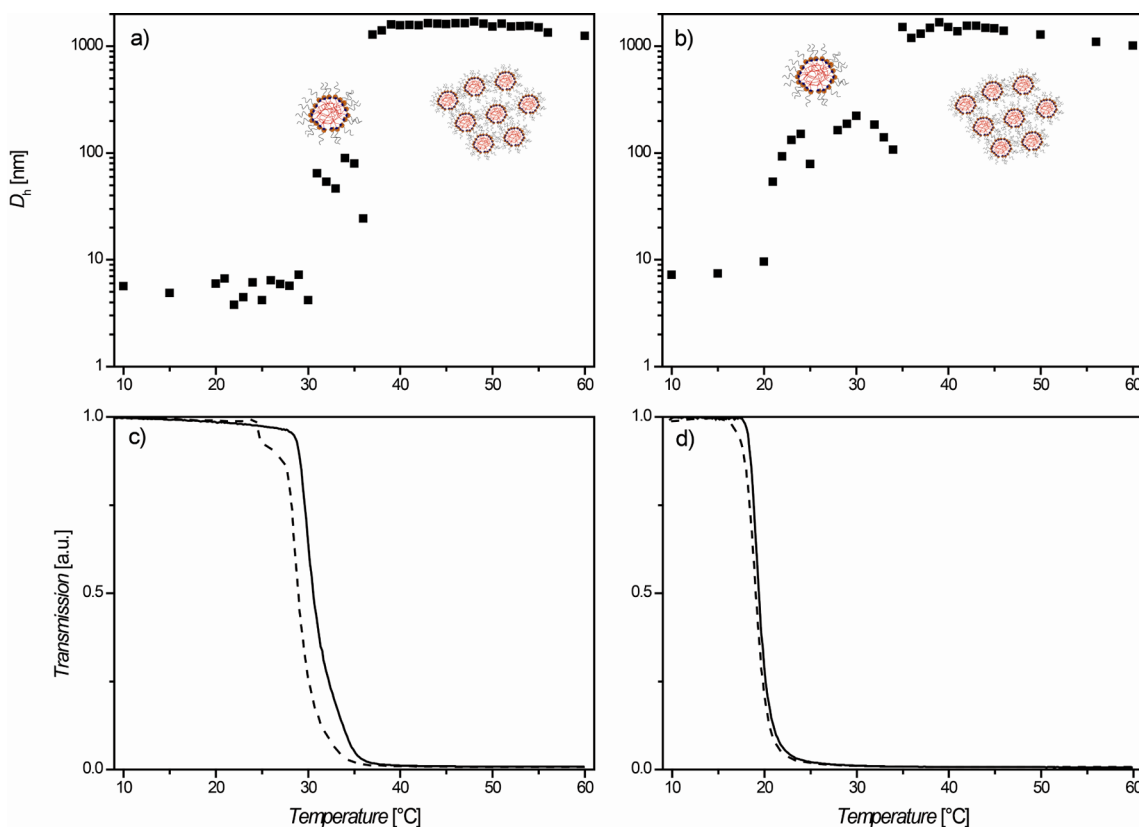


**Figure 6.** (a) Temperature sequenced DLS measurement of PDEAAm<sub>78</sub>Ad<sub>2</sub>-*b*-(PHPMA<sub>28</sub>- $\beta$ -CD)<sub>2</sub> at a heating rate of 0.2 °C min<sup>-1</sup> and a concentration of 1 mg mL<sup>-1</sup>. (b) Temperature sequenced DLS measurement of PDEAAm<sub>59</sub>Azo<sub>2</sub>-*b*-(PHPMA<sub>28</sub>- $\beta$ -CD)<sub>2</sub> at a heating rate of 0.2 °C min<sup>-1</sup> and a concentration of 1 mg mL<sup>-1</sup>. (c) Turbidity measurements for PDEAAm<sub>78</sub>Ad<sub>2</sub> (dashed line) and the supramolecular triblock copolymer PDEAAm<sub>78</sub>Ad<sub>2</sub>-*b*-(PHPMA<sub>28</sub>- $\beta$ -CD)<sub>2</sub> (solid line) at a cooling rate of 0.32 °C min<sup>-1</sup> and a concentration of 1 mg mL<sup>-1</sup>. (d) Turbidity measurements for PDEAAm<sub>59</sub>Azo<sub>2</sub> (dashed line) and the supramolecular triblock copolymer PDEAAm<sub>59</sub>Azo<sub>2</sub>-*b*-(PHPMA<sub>28</sub>- $\beta$ -CD)<sub>2</sub> (solid line) at a cooling rate of 0.32 °C min<sup>-1</sup> and a concentration of 1 mg mL<sup>-1</sup>.

weight polymers and the earlier mentioned aggregates disturb the complex re-formation.

In addition to the thermoresponsivity of the employed host/guest complexes, azobenzenes provide the opportunity to generate structures that are sensitive to light irradiation as azobenzenes show a transition from the thermodynamically more stable *trans*- to the *cis*-conformation at wavelengths close to 360 nm. This photoisomerization is reversible and the re-isomerization can be induced by heat or light with wavelengths of close to 430 nm. Furthermore, the complexation constants are higher for the *trans*-conformation compared to the *cis*-conformation (460 M<sup>-1</sup> for a *trans*-azobenzene test compound and 2.5 M<sup>-1</sup> for a *cis*-azobenzene test compound).<sup>53</sup> In general, higher complexation constants (up to 10<sup>4</sup> M<sup>-1</sup>)<sup>54</sup> and differences between *cis*- and *trans*-conformations could be achieved via the utilization of  $\alpha$ -CD instead of  $\beta$ -CD. In here, azobenzene-based  $\beta$ -CD complexes were irradiated with UV light at 350 nm for 30 min, and the change in  $D_h$  was monitored via DLS. A significant decrease was evident, e.g., from 8.9 to 4.8 nm after irradiation in the case of PDEAAm<sub>80</sub>Azo<sub>2</sub>-*b*-(PHPMA<sub>28</sub>- $\beta$ -CD)<sub>2</sub> (see Figure S<sub>c,d</sub>, Table S13, and Figure S29), evidencing that the block copolymers are debonded in a photoresponsive fashion. After keeping the samples at ambient temperature and daylight, the block copolymers formed again as proven by an increased  $D_h$  value, e.g., 8.2 nm compared to the original value of 8.9 nm in the case of PDEAAm<sub>80</sub>Azo<sub>2</sub>-*b*-(PHPMA<sub>28</sub>- $\beta$ -CD)<sub>2</sub> and 10.1 nm compared to 11.2 nm before in the case of PDMAAm<sub>103</sub>Azo<sub>2</sub>-*b*-

(PHPMA<sub>26</sub>- $\beta$ -CD)<sub>2</sub>. In almost all cases the  $D_h$  after standing in daylight is close to the initial value. As shown in Figure S<sub>b,d</sub>, the azobenzene-based PDMAAm block copolymers are dual responsively bound as their supramolecular connection is sensitive to heat and light. The light triggered complex dissociation could be observed furthermore via 2D NOESY NMR (see Figure 4d and an overlay in Figure S30). The intensity of the corresponding cross-correlation peaks decreases significantly after irradiation of UV light for 7 min. Nevertheless, the peaks do not vanish completely. This can be attributed to the fact that the complexes could re-form during the NOESY measurement with a measuring time of around 9 h. Furthermore, an equilibrium between *cis*- and *trans*-azobenzenes is formed where small amounts of *trans*-azobenzenes with higher complexation constant remain in the solution and the irradiation time is limited as RAFT polymers are sensitive to UV irradiation. The formation of *cis*-azobenzenes can be monitored via UV spectroscopy as well. The UV spectra of all samples show a significant increase of the absorption at 440 nm after irradiation at 350 nm for 30 min (see Figures S31–33). Concomitantly, the absorption of *trans*-azobenzene moieties at 340 nm decreases drastically. As the absorption of *trans*-azobenzene is overlapping with the absorption of the trithiocarbonate, a quantitative statement with respect to the *trans*- and *cis*-azobenzene content in solution is difficult. Nevertheless, judging from the shape of the absorption band after irradiation, only minor amounts of *trans*-azobenzene remain.

The utilization of PDEAAm as inner block provides the opportunity for temperature-induced aggregation.<sup>21,34,35,37</sup> As shown in Figure 6, the block copolymers are present as random coils at lower temperatures, e.g., a  $D_h$  of around 7 nm for PDEAAm<sub>78</sub>Ad<sub>2</sub>-*b*-(PHPMA<sub>28</sub>- $\beta$ -CD)<sub>2</sub> up to 30 °C or a  $D_h$  around 8 nm for PDEAAm<sub>59</sub>Azo<sub>2</sub>-*b*-(PHPMA<sub>28</sub>- $\beta$ -CD)<sub>2</sub> up to 20 °C (Figure 6a,b). The situation changes upon heating over the cloud point where aggregates are formed. In the case of PDEAAm<sub>78</sub>Ad<sub>2</sub>-*b*-(PHPMA<sub>28</sub>- $\beta$ -CD)<sub>2</sub> aggregates with  $D_h$  between 24 and 90 nm are formed between 31 and 36 °C. A broader temperature range from 21 to 34 °C is covered with PDEAAm<sub>59</sub>Azo<sub>2</sub>-*b*-(PHPMA<sub>28</sub>- $\beta$ -CD)<sub>2</sub>, where  $D_h$  between 54 and 222 nm are observed (refer to Figure S34 and Table S14 for further examples and information). With further heating these aggregates agglomerate leading to particles with sizes over 1000 nm in all cases except of PDEAAm<sub>36</sub>Azo<sub>2</sub>-*b*-(PHPMA<sub>28</sub>- $\beta$ -CD)<sub>2</sub> where particles between 500 and 1000 nm are found. The behavior of these triblock copolymers resembles the behavior of literature known systems where a plateau as well as further agglomeration is described.<sup>21,35,37</sup> One possible explanation for agglomeration at higher temperatures is the decreased complex stability, making a dynamic exchange of the building blocks possible. Thus, the stabilization effect of the PHPMA corona on the PDEAAm cores is decreasing and finally the aggregates begin to agglomerate. The DLS data are in agreement with the plots of turbidimetry as evident via the direct comparison in Figures 6a,c and 6b,d.

Turbidity measurements show in almost all cases an increased cloud point of the complexes compared to the uncomplexed PDEAAm blocks (refer to Figure 6, Figure S35, and Table S15), which is an expected behavior of supramolecular block copolymers with a thermoresponsive block.<sup>19,21,35,37</sup> A possible explanation for such a behavior is the shielding of the hydrophobic end groups by the CD moiety. In the case of doubly adamantyl-functionalized polymers the difference in the cloud points lies between 4 and 2 °C, whereas the difference with azobenzene-functionalized polymers is rather small and the cloud points are almost the same. A reason for the different behavior of the guest groups may be the enhanced polarity of the azobenzene moiety and the weaker association with  $\beta$ -CD. Furthermore, an increase of the cloud point with molecular weight is evident as well.

## CONCLUSIONS

We present the synthesis of a novel macromolecular architecture based on CD host/guest chemistry, i.e., an ABA triblock copolymer. A doubly guest-functionalized, namely adamantyl- and azobenzene-functionalized inner block, was synthesized via RAFT polymerization of DMAAm and DEAAm. The host functionalized block was synthesized via RAFT polymerization of the monomer HPMA, affording the biocompatible PHPMA, and a CuAAC conjugation with  $\beta$ -CD-N<sub>3</sub>. The individual blocks were characterized via SEC, <sup>1</sup>H NMR, and ESI-MS. Subsequently, the triblock copolymers were formed in aqueous solution, and the complex formation was evidenced via DLS, 2D NOESY NMR, and turbidity measurements. Furthermore, the triblock copolymer formation was responsive to temperature and in the case of azobenzene guests to irradiation of light at 350 nm in a reversible fashion as disassembly after the stimuli and reassembly of the triblock copolymers was unambiguously evidenced. In the case of PDEAAm, the temperature-induced aggregation was inves-

tigated after heating above the cloud point of the PDEAAm block.

## ASSOCIATED CONTENT

### Supporting Information

Analytical data of the chain transfer agents and other synthesized molecules, additional experimental data on the obtained polymers and the supramolecular complexes; additional experimental procedures on the synthesis of HPMA and the chain transfer agent precursors. This material is available free of charge via the Internet at <http://pubs.acs.org>.

## AUTHOR INFORMATION

### Corresponding Author

\*Tel (+49) 721 608-45642, Fax (+49) 721 608-45740, e-mail [christopher.barner-kowollik@kit.edu](mailto:christopher.barner-kowollik@kit.edu) (C.B.-K.); Tel (+49) 211 81-14760, Fax (+49) 211 81-15840, e-mail [h.ritter@uni-duesseldorf.de](mailto:h.ritter@uni-duesseldorf.de) (H.R.).

### Notes

The authors declare no competing financial interest.

## ACKNOWLEDGMENTS

The authors acknowledge financial support for the current project from the German Research Council (DFG). C.B.-K. acknowledges additional financial support from the Karlsruhe Institute of Technology (KIT) in the context of the Excellence Initiative for leading German universities and the Ministry for Science and Arts of the state of Baden-Württemberg. The authors acknowledge Prof. Dr. Luy (KIT) for helpful discussions.

## REFERENCES

- (1) Ruzette, A.-V.; Leibler, L. *Nat. Mater.* **2005**, *4* (1), 19–31.
- (2) Lodge, T. P. *Macromol. Chem. Phys.* **2003**, *204* (2), 265–273.
- (3) Ishizone, T.; Hirao, A. Anionic Polymerization: Recent Advances. In *Synthesis of Polymers: New Structures and Methods*; Schlüter, A. D., Hawker, C. J., Sakamoto, J., Eds.; Wiley-VCH: Weinheim, 2012; pp 81–134.
- (4) Aoshima, S.; Kanaoka, S. *Chem. Rev.* **2009**, *109* (11), 5245–5287.
- (5) Hawker, C. J.; Bosman, A. W.; Harth, E. *Chem. Rev.* **2001**, *101* (12), 3661–3688.
- (6) Ouchi, M.; Terashima, T.; Sawamoto, M. *Chem. Rev.* **2009**, *109* (11), 4963–5050.
- (7) Matyjaszewski, K. *Macromolecules* **2012**, *45* (10), 4015–4039.
- (8) Barner-Kowollik, C. *Handbook of RAFT-Polymerization*; Wiley-VCH: Weinheim, Germany, 2008.
- (9) Chiefari, J.; Chong, Y. K.; Ercole, F.; Krstina, J.; Jeffery, J.; Le, T. P. T.; Mayadunne, R. T. A.; Meijs, G. F.; Moad, C. L.; Moad, G.; Rizzardo, E.; Thang, S. H. *Macromolecules* **1998**, *31* (16), 5559–5562.
- (10) Barner-Kowollik, C.; Inglis, A. J. *Macromol. Chem. Phys.* **2009**, *210* (12), 987–992.
- (11) Lutz, J. F. *Angew. Chem., Int. Ed.* **2007**, *46* (7), 1018–1025.
- (12) Kempe, K.; Krieg, A.; Becer, C. R.; Schubert, U. S. *Chem. Soc. Rev.* **2012**, *41* (1), 176–191.
- (13) Opsteen, J. A.; van Hest, J. C. M. *Chem. Commun.* **2005**, *1*, 57–59.
- (14) Hizal, G.; Tunca, U.; Sanyal, A. *J. Polym. Sci., Part A: Polym. Chem.* **2011**, *49* (19), 4103–4120.
- (15) Inglis, A. J.; Stenzel, M. H.; Barner-Kowollik, C. *Macromol. Rapid Commun.* **2009**, *30* (21), 1792–1798.
- (16) Durmaz, H.; Hizal, G.; Tunca, U. *J. Polym. Sci., Part A: Polym. Chem.* **2011**, *49* (9), 1962–1968.
- (17) Schmidt, B. V. K. J.; Fechner, N.; Falkenhagen, J.; Lutz, J.-F. *Nat. Chem.* **2011**, *3* (3), 234–238.
- (18) Chen, G.; Jiang, M. *Chem. Soc. Rev.* **2011**, *40* (5), 2254–2266.

- (19) Schmidt, B. V. K. J.; Rudolph, T.; Hetzer, M.; Ritter, H.; Schacher, F. H.; Barner-Kowollik, C. *Polym. Chem.* **2012**, *3* (11), 3139–3145.
- (20) Zhang, Q.; Li, G.-Z.; Becer, C. R.; Haddleton, D. M. *Chem. Commun.* **2012**, *48* (65), 8063–8065.
- (21) Schmidt, B. V. K. J.; Hetzer, M.; Ritter, H.; Barner-Kowollik, C. *Polym. Chem.* **2012**, *3* (11), 3064–3067.
- (22) Huan, X.; Wang, D.; Dong, R.; Tu, C.; Zhu, B.; Yan, D.; Zhu, X. *Macromolecules* **2012**, *45* (15), 5941–5947.
- (23) Nakahata, M.; Takashima, Y.; Yamaguchi, H.; Harada, A. *Nat. Commun.* **2011**, *2*, 511.
- (24) Bertrand, A.; Stenzel, M.; Fleury, E.; Bernard, J. *Polym. Chem.* **2012**, *3* (2), 377–383.
- (25) Köllisch, H. S.; Barner-Kowollik, C.; Ritter, H. *Chem. Commun.* **2009**, *9*, 1097–1099.
- (26) Köllisch, H.; Barner-Kowollik, C.; Ritter, H. *Macromol. Rapid Commun.* **2006**, *27* (11), 848–853.
- (27) Ritter, H.; Mondrzyk, B. E.; Rehahn, M.; Gallei, M. *Beilstein J. Org. Chem.* **2010**, *6*.
- (28) Ding, L.; Li, Y.; Deng, J.; Yang, W. *Polym. Chem.* **2011**, *2* (3), 694–701.
- (29) Schmidt, B. V. K. J.; Hetzer, M.; Ritter, H.; Barner-Kowollik, C. *Macromolecules* **2011**, *44* (18), 7220–7232.
- (30) Harada, A.; Kobayashi, R.; Takashima, Y.; Hashidzume, A.; Yamaguchi, H. *Nat. Chem.* **2011**, *3* (1), 34–37.
- (31) Yan, Q.; Xin, Y.; Zhou, R.; Yin, Y.; Yuan, J. *Chem. Commun.* **2011**, *47* (34), 9594–9596.
- (32) Yan, Q.; Yuan, J.; Cai, Z.; Xin, Y.; Kang, Y.; Yin, Y. *J. Am. Chem. Soc.* **2010**, *132* (27), 9268–9270.
- (33) Stadermann, J.; Komber, H.; Erber, M.; Däbritz, F.; Ritter, H.; Voit, B. *Macromolecules* **2011**, *44* (9), 3250–3259.
- (34) Zeng, J.; Shi, K.; Zhang, Y.; Sun, X.; Zhang, B. *Chem. Commun.* **2008**, *32*, 3753–3755.
- (35) Liu, H.; Zhang, Y.; Hu, J.; Li, C.; Liu, S. *Macromol. Chem. Phys.* **2009**, *210* (24), 2125–2137.
- (36) Zhang, Z.-X.; Liu, X.; Xu, F. J.; Loh, X. J.; Kang, E.-T.; Neoh, K.-G.; Li, J. *Macromolecules* **2008**, *41* (16), 5967–5970.
- (37) Zhang, Z.-X.; Liu, K. L.; Li, J. *Macromolecules* **2011**, *44* (5), 1182–1193.
- (38) Yhaya, F.; Binauld, S.; Callari, M.; Stenzel, M. H. *Aust. J. Chem.* **2012**, *65* (8), 1095–1103.
- (39) Quan, C.-Y.; Chen, J.-X.; Wang, H.-Y.; Li, C.; Chang, C.; Zhang, X.-Z.; Zhuo, R.-X. *ACS Nano* **2010**, *4* (7), 4211–4219.
- (40) Rao, J.; Paunescu, E.; Mirmohades, M.; Gadwal, I.; Khaydarov, A.; Hawker, C. J.; Bang, J.; Khan, A. *Polym. Chem.* **2012**, *3* (8), 2050–2056.
- (41) Fleige, E.; Quadir, M. A.; Haag, R. *Adv. Drug Delivery Rev.* **2012**, *64* (9), 866–884.
- (42) Gan, L. H.; Cai, W.; Tam, K. C. *Eur. Polym. J.* **2001**, *37* (9), 1773–1778.
- (43) Skey, J.; O'Reilly, R. K. *Chem. Commun.* **2008**, *35*, 4183–4185.
- (44) Lai, J. T.; Filla, D.; Shea, R. *Macromolecules* **2002**, *35* (18), 6754–6756.
- (45) Moad, G.; Chong, Y. K.; Postma, A.; Rizzardo, E.; Thang, S. H. *Polymer* **2005**, *46* (19), 8458–8468.
- (46) Apostolovic, B.; Deacon, S. P. E.; Duncan, R.; Klok, H.-A. *Biomacromolecules* **2010**, *11* (5), 1187–1195.
- (47) Amajjahe, S.; Choi, S.; Munteanu, M.; Ritter, H. *Angew. Chem., Int. Ed.* **2008**, *47* (18), 3435–3437.
- (48) Li, C.; Lo, C.-W.; Zhu, D.; Li, C.; Liu, Y.; Jiang, H. *Macromol. Rapid Commun.* **2009**, *30* (22), 1928–1935.
- (49) Kwak, R. N. Y.; Matyjaszewski, K. *Macromolecules* **2008**, *41* (13), 4585–4596.
- (50) Rekharsky, M. V.; Inoue, Y. *Chem. Rev.* **1998**, *98* (5), 1875–1918.
- (51) Ross, P. D.; Rekharsky, M. V. *Biophys. J.* **1996**, *71* (4), 2144–2154.
- (52) Del Valle, E. M. M. *Process Biochem.* **2004**, *39* (9), 1033–1046.
- (53) Takashima, Y.; Nakayama, T.; Miyauchi, M.; Kawaguchi, Y.; Yamaguchi, H.; Harada, A. *Chem. Lett.* **2004**, *33*, 890–891.
- (54) Tomatsu, I.; Hashidzume, A.; Harada, A. *Macromolecules* **2005**, *38* (12), 5223–5227.